

Degree of accuracy in determining the nuclear electric quadrupole moment of radium

Jacek Bieroń¹ and Pekka Pyykkö²¹*Instytut Fizyki imienia Mariana Smoluchowskiego, Uniwersytet Jagielloński, Reymonta 4, 30-059 Kraków, Poland*²*Department of Chemistry, University of Helsinki, P. O. Box 55 (A.I. Virtasen aukio 1), 00014 Helsinki, Finland*

(Received 13 December 2004; published 9 March 2005)

The multiconfiguration Dirac-Hartree-Fock (MCDHF) model has been employed to calculate the atomic expectation values responsible for the hyperfine splittings of the $7s7p\ ^3P_{1,2}$ and 1P_1 levels of radium. Calculated electric field gradients, together with the experimental electric quadrupole hyperfine structure constants, allow us to extract a nuclear electric quadrupole moment $Q(^{223}\text{Ra})$ of 1.21(0.03) barn. This value is in good agreement with the semiempirical determination based on neutral radium hyperfine and fine structure, but differs from the latest result from an alkali-like radium ion.

DOI: 10.1103/PhysRevA.71.032502

PACS number(s): 31.15.Ar, 31.30.Jv, 31.30.Gs, 21.10.Ky

I. INTRODUCTION

The nuclear electric quadrupole moment constitutes an indication of a nuclear charge asymmetry, which is important in atomic, molecular, and solid-state spectroscopy, and in nuclear physics [1]. Radium has recently become a subject of theoretical [2] and experimental [3] investigations aimed at the detection of permanent electric dipole moments of elementary particles [4], associated with the possible violation of time-reversal invariance [5,6]. The advantage of radium lies in octupole deformations of nuclei in several isotopes [7], simple electronic structure $[\text{Kr}]4d^{10}4f^{14}5s^25p^65d^{10}6s^26p^67s^2$, as well as in coincidental proximity of two atomic levels of opposite parity, $7s7p\ ^3P_1$ and $7s6d\ ^3D_2$, which are separated by a very small energy interval 5 cm^{-1} . The data on the atomic spectrum of radium, compiled in the tables of Moore [8], came from the experimental investigations of Rasmussen [9], with subsequent revisions by Russell [10]; both go back to the 1930s. The experimental investigations of the hyperfine structures of radium have been performed by the group of Wendt [11–16] in the 1980s. They have studied both atomic Ra I as well as ionic Ra II spectra, and obtained isotope shifts and hyperfine parameters for several states. In particular, in their 1987 paper [12] they determined the magnetic dipole hyperfine constants A , as well as electric quadrupole constants B , for the $7s7p\ ^1P_1$, $7s7p\ ^3P_1$, $7s7p\ ^3P_2$, and $7s7d\ ^3D_3$ levels of neutral radium. Based on a semiempirical evaluation of the radial parameter $\langle r^{-3} \rangle$, they arrived at the nuclear quadrupole moment $Q=1.19(12)$ for the isotope Ra-223. Two years later, they were also able to reach into the ultraviolet region, and from the $7s\ ^2S_{1/2}-7p\ ^2P_{3/2}$ line of the alkali-like Ra II they derived [15] a more accurate value of the nuclear quadrupole moment $Q=1.254(3)\{66\}$ for the Ra-223 isotope. The number in curly brackets reflects the “scaling uncertainty” of their semiempirical analysis, i.e., the estimate of the accuracy of their evaluation of the electric field gradients, and in particular the relativistic and Sternheimer corrections. Hyperfine structures of singly ionized radium have also been the subject of several theoretical papers [17–22].

In the present paper, we performed large-scale multiconfiguration Dirac-Hartree-Fock (MCDHF) calculations of the

magnetic fields and the electric field gradients generated by the electronic cloud in the $7s7p\ ^1P_1$, $7s7p\ ^3P_1$, and $7s7p\ ^3P_2$ states of the neutral Ra-223 isotope. Combined with the measurements of the electric quadrupole constants B published by Wendt *et al.* [12], we obtain three independently determined values of the nuclear quadrupole moment $Q(^{223}\text{Ra})$.

The purpose of the paper is threefold. First, we performed an *ab initio* evaluation of the nuclear electric quadrupole moment of radium-223. Our final result $Q(^{223}\text{Ra})=1.21(0.03)$ fits, within the error limits, the value $Q=1.254(3)\{66\}$ published in the latest paper by the group of Wendt (Neu *et al.* [15]), but is about 4% smaller. Our value seems to be closer to the earlier, less accurate result of Wendt *et al.* [12], derived from the measurement of hyperfine structure of the neutral radium. A second purpose of the present paper was to narrow the relatively large error bars of the previous determinations. This target has been achieved only partially. The three values of our calculated nuclear quadrupole moment $Q(^{223}\text{Ra})$, derived from three independent calculations, are in almost 1% agreement, and one might reasonably expect that the final accuracy would be of a similar order. However, as a check of the quality of the calculated wave functions, we evaluated the magnetic dipole hyperfine constants A for the same three levels of radium, and compared them with the experimental results of Wendt *et al.* [12]. All three calculated values differ from the experimental values by about 5% (see Table II). Full analysis of the error limits is presented in Sec. IV of the present paper. Another route to improve the accuracy of the final value of $Q(^{223}\text{Ra})$ would be to increase the number of different levels, for which the B values were measured experimentally. Except for the $7s7d\ ^3D_3$ level, which is in fact difficult to access computationally, there are also four lower-lying levels of D symmetry in the spectrum of radium, all of which belong to the $7s6d$ configuration. Therefore, the third purpose of the present paper is to draw the attention of the experimenters to the need of hyperfine structure constants A and B for the $7s6d\ ^1D_2$, $7s6d\ ^3D_3$, $7s6d\ ^3D_2$, and $7s6d\ ^3D_1$ levels of radium.

In Sec. II, we briefly describe the MCDHF theory [23,24]. Then in Sec. III, the method is presented in some detail, followed by a discussion of the results in Sec. IV and conclusions in Sec. V. The practical implementation [25,26] of

the Dirac-Fock code and a through introduction to the method of calculation [27–30] have been described elsewhere. A similar method has been used to determine the nuclear electric quadrupole moments of other heavy elements, such as Br, I [31], Bi [32], and Hg [33].

II. THEORY

The atomic wave function Ψ for a particular atomic state Γ ,

$$\Psi(\Gamma PJM) = \sum_r^{\text{NCF}} c_r \Phi(\gamma_r PJM), \quad (1)$$

is obtained as the self-consistent solution of Dirac-Fock equations [23] in systematically [27,32] increased multiconfiguration basis of NCF (i.e., number of configuration functions) symmetry-adapted eigenfunctions of J^2, J_z , and parity P . Configuration mixing coefficients c_r are obtained through diagonalization of the Dirac-Coulomb Hamiltonian,

$$H_{\text{DC}} = \sum_i c \alpha_i \cdot \mathbf{p}_i + (\beta_i - 1)c^2 - Z/r_i + \sum_{i>j} 1/r_{ij}. \quad (2)$$

The effects of the Breit interaction have been estimated in separate configuration-interaction calculations, where the matrix elements of the Breit operator at the low-frequency limit

$$B_{ij} = -\frac{1}{2r_{ij}} \left[\alpha_i \cdot \alpha_j + \frac{(\alpha_i \cdot \mathbf{r}_{ij})(\alpha_j \cdot \mathbf{r}_{ij})}{r_{ij}^2} \right] \quad (3)$$

were evaluated perturbatively, as described in [34]. The QED effects included the anomalous magnetic moment of the electron, for which the factor $g_s/2 = 1.001\,159\,652\,19$ has been used [35], vacuum polarization, and self-energy (evaluated using the Z_{eff} approach in GRASP [34]). Finally, the coefficients c_r , together with one-electron orbital sets, provided the numerical representations of the $7s7p\ ^1P_1, 7s7p\ ^3P_1$, and $7s7p\ ^3P_2$ states of neutral radium. The expectation values of magnetic fields and electric field gradients were evaluated with the HFS92 program [26]. The evaluation of the nuclear quadrupole moment is based on the calculated value of the electric field gradient generated by the electronic cloud, and on the experimentally determined hyperfine splitting of the atomic energy level. The electric quadrupole part of the hyperfine shift of the atomic level $\Psi(\Gamma PJM)$ is usually expressed in terms of the electric quadrupole hyperfine constant $B(\Gamma PJM)$, which depends on the nuclear electric quadrupole moment Q and the electric field gradient q in the state $\Psi(\Gamma PJM)$, through the equation

$$B(\Gamma PJM) = eq(\Gamma PJM)Q/h. \quad (4)$$

The hyperfine structure Hamiltonian [26] assumes pointlike nuclear magnetic dipole moments. The correction arising from spatial distribution of the magnetic moment inside the nucleus (the Bohr-Weisskopf [36] effect) depends primarily on the radial shape of the magnetization distribution inside the nucleus. In even-odd isotopes, the magnetic moment is often largely due to the unpaired neutron, and therefore the

$^{223}_{88}\text{Ra}$ nucleus may be expected to possess the following characteristics: (i) high surface concentration of the magnetization distribution, as opposed to a more uniform volume distribution of the electric charge; (ii) the magnetic radius $\langle r_m^2 \rangle^{1/2}$ larger than the electric charge radius $\langle r_c^2 \rangle^{1/2}$. The latter feature has also been observed in the odd-odd $^{208}_{87}\text{Cs}$, $^{210}_{87}\text{Cs}$, and $^{212}_{87}\text{Cs}$ isotopes [37], as well as in the odd-even $^{185}_{75}\text{Re}$ and $^{187}_{75}\text{Re}$ isotopes [38]. To our knowledge, neither the magnetization distribution nor the magnetic radius is known for any isotope of radium. Therefore, we employed the $1 - \epsilon = 0.96$ correction evaluated with the procedure developed by Kopfermann [39]. In light of the uncertainties mentioned above, this correction should be regarded as a rather crude estimate, but the magnetic dipole hyperfine structure is not the primary objective of the present paper. The value of the nuclear magnetic dipole moment for the $^{223}_{88}\text{Ra}$ isotope was taken from the tables of Raghavan [40].

III. METHOD

The generation of wave functions followed the scheme described in our previous papers [33,41]. All radial orbitals, as well as mixing coefficients [c_r in Eq. (1)], were separately optimized for each of the three states of interest, i.e., $^1P_1, ^3P_1$, and 3P_2 . The multiconfiguration expansions were generated within systematically enlarged [27,32] sets of virtual orbitals, yielding increasingly accurate approximations to the exact wave functions. In each case (i.e., for each state), the computation process was divided into four phases. In the first phase, the spectroscopic orbitals required to form a reference wave function were obtained with a minimal configuration expansion, with full relaxation.

In the second phase, the virtual orbitals were generated in five consecutive steps. At each step the virtual set was extended by one layer of virtual orbitals. A layer is defined as a set of virtual orbitals with different angular symmetries. In the present paper, five layers of virtual orbitals of each of the s, p, d, f, g, h symmetries were generated. At each step the configuration expansions were limited to single and double substitutions from valence shells to all new orbitals and to all previously generated virtual layers (this is essentially the valence correlation approximation). These configuration expansions were augmented by a small subset of dominant single and double substitutions from core ($5s5p5d6s6p$) and valence ($7s7p$) shells, with the further restriction that at most one electron may be promoted from core shells (which means that in the case of a double substitution, the second electron must be promoted from a valence shell). All configurations from earlier steps were retained, with all previously generated orbitals fixed, and all new orbitals were made orthogonal to others of the same symmetry. The initial shapes of radial orbitals were obtained in the Thomas-Fermi potential, and then driven to convergence with the self-consistency threshold set to 10^{-8} . All calculations were done with a spherical variable-density model for the nuclear electric charge distribution. A two-parameter Fermi function [42] was employed to describe the radial charge distribution.

In the third phase, the configuration-interaction calculations (i.e., with no changes to the radial wave functions)

were performed, with multiconfiguration expansions tailored in such a way as to capture the core polarization, which is the leading electron correlation contribution to the hyperfine expectation values [18,43,44]. All single and double substitutions were allowed from several core shells and all valence shells (i.e., $7s$, $7p-$, and $7p+$) to all virtual shells, with the same restriction as above, i.e., that at most one electron may be promoted from core shells (this is core polarization, or core-valence approximation). The virtual set was systematically increased from one to five layers. At each step, i.e., for each intermediate set of layers, several core shells were correlated—electron substitutions were allowed from the outermost $6p$ core shell at first, then from $6s6p$, and so on, until the largest open-core calculation, where substitutions were allowed from $4s4p4d4f5s5p5d6s6p$ shells. Opening the $n=4$ shells together brought about the 0.3% relative change of the calculated value of the electric field gradient and the 0.1% change of the calculated magnetic field for the 1P_1 state. Therefore, in all subsequent calculations the $n=4$ and all deeper lying shells were kept closed. During generation of the sixth layer, convergence problems were encountered with the s symmetry orbital. The presence of the fifth layer in the virtual orbital set brought about a 0.6% relative change of the calculated value of the electric field gradient and a 1.8% change of the calculated magnetic field for the 1P_1 state. Based on our earlier hyperfine structure calculations [27,45], and on similar conclusions by other authors [19,21], we estimated that the contribution to the hyperfine fields arising from the omitted sixth layer and all other omitted virtual shells does not exceed 1% in the case of the magnetic hyperfine field and much less in the case of the electric field gradient.

In the fourth phase of the wave-function generation, the core-core correlation effects were estimated in two (for each of the three levels) large-scale configuration-interaction calculations. First, the core $6p$ shell was opened for double substitutions to the first layer of virtual orbitals. These configurations were augmented by the final core-valence expansion. In the second step, the double substitutions from the core $6s6p$ shells were allowed to one layer of virtual orbitals and again augmented by the final core-valence expansion. The computer constraints did not permit any further extension of the double substitutions. Each of the several largest configuration-interaction calculations performed in this study took more than a week on an eight-node cluster of Linux machines of 13 GHz total peak power, and required up to 100 GB temporary disk storage for the Hamiltonian matrix. Any meaningful extension of the correlation model would require an order of magnitude increase of the computing power. As the very last phase of the calculations, Breit and QED corrections are estimated with the method described in [45], whereby both corrections are evaluated perturbatively and monitored along a systematically enlarged multiconfiguration expansion, until saturation with respect to the size of the expansion is obtained.

IV. RESULTS

Table I presents the values of the nuclear electric quadrupole moment Q derived from the calculated values of the

TABLE I. *Ab initio* values of the nuclear electric quadrupole moment Q (barn) of ^{223}Ra derived from the experimental electric quadrupole hyperfine structure constants B and from the calculated electric field gradients for the $7s7p^1P_1$, 3P_1 , 3P_2 levels of radium, in several different approximations: DF, uncorrelated Dirac-Fock; vv, valence correlation included; cv, core-valence correlation included; cc, core-core correlation included.

	1P_1	3P_1	3P_2
DF	1.9914	1.8469	2.1414
vv	2.4037	1.9262	2.1207
cv+vv	1.1931	1.1913	1.2199
cc+cv+vv	1.1925	1.1797	1.2076
Breit & QED	0.0257	0.0140	0.0030
total	1.218	1.194	1.211

electric field gradient for the $7s7p^1P_1$, 3P_1 , 3P_2 levels of ^{223}Ra .

Since they were determined in three independent calculations for three different atomic levels, it would be reasonable to assume the statistical distribution (rather than systematic deviation) of computed values of Q , which would allow us to treat their variance in a similar manner as a purely statistical “experimental” error distribution. Such a procedure would yield the value $Q(^{223}\text{Ra})=1.208(0.008)$. There are, however, two objections. First, the sample is too small for any reasonable level of confidence. It would be highly desirable to perform similar calculations on a larger sample. As indicated in the Introduction, we would like to encourage the experimenters to measure the hyperfine structures and B constants for other levels of radium.

The second objection arises upon inspection of Table II, where the calculated values of the magnetic dipole hyperfine structure constants A of the $7s7p^1P_1$, 3P_1 , and 3P_2 levels of ^{223}Ra are presented. The comparison with experiment shows that all three calculated constants deviate from experiment

TABLE II. Calculated values of the magnetic dipole hyperfine structure constants A (MHz) of the $7s7p^1P_1$, 3P_1 , and 3P_2 levels of ^{223}Ra , compared with experiment; DF, uncorrelated Dirac-Fock; vv, valence correlation included; cv, core-valence correlation included; cc, core-core correlation included. Experimental data are quoted from the paper by Wendt *et al.* [12]. The RCI+RPA entry is calculated from the value published by Dzuba *et al.* [46].

	1P_1	3P_1	3P_2
DF	-226.59	803.97	567.22
vv	-216.41	873.50	547.19
cv+vv	-363.65	1336.94	785.58
cc+cv+vv	-351.21	1329.02	779.09
Breit & QED	7.15	-24.92	-11.24
BW	13.76	-52.20	-30.76
total	-330.3	1251.9	737.1
experiment	-344.5(0.9)	1201.1(0.6)	699.6(3.3)
RCI+RPA	-242.4		

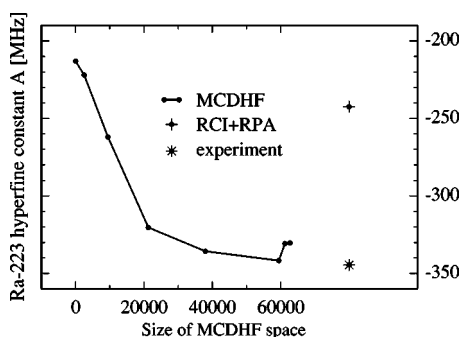


FIG. 1. Hyperfine magnetic dipole constant A of the $7s7p\ ^1P_1$ state of the radium-223 isotope as a function of the number of configuration functions in the multiconfiguration expansion, compared with experiment [12] and other theory [46].

by about 5%. The disagreement probably arises from higher-order correlation effects, which for the time being remain beyond the reach of the computer systems at our disposal. As described in Sec. III, the final, largest configuration-interaction calculations were composed from (i) final core-valence expansion and (ii) double substitutions from the core $6s6p$ shells to one layer of virtual orbitals, which generated 92 921 relativistic configurations for the 3P_2 state and 62 751 for each of the other two states.

Figure 1 presents the calculated hyperfine magnetic dipole constant A for the $7s7p\ ^1P_1$ state as a function of the number of configuration functions in the multiconfiguration expansion. An interesting, albeit unexplained, feature is the almost complete absence of oscillations in the function $A(\text{NCF})$ (where NCF represents the size of the MCDHF expansion). An oscillatory behavior of $A(\text{NCF})$ has often been observed in multiconfiguration Dirac- and Hartree-Fock calculations [27,32,33,44]. The monotonic, decreasing part of the curve shows the core-valence results. It appears to be almost fully converged, while the same cannot be said about the last two points, which represent the final core-core calculations. The core-core model adopted in this paper should capture the large part of core-core correlation effects, but certainly does not achieve saturation, and constitutes the largest source of uncertainty in the present calculations. There exist indications in the literature [18–20,22] that for the Ra^+ ion, the core-core correlation effects amount to about 20% of the total value of the hyperfine shift in the magnetic dipole hyperfine structure calculations. In particular, a non-negligible contribution may arise due to double substitutions from the $5d$ shell, which were not accounted for in the present study (a 4% contribution in the case of the magnetic dipole hyperfine constant A for the $^2P_{3/2}$ level of $^{221}\text{Ra}^+$ ion was reported by Yuan *et al.* [22]). The core-polarization (core-valence correlation) effects were also reported to reach about 20% of the total value of the hyperfine shift for the excited $^2P_{1/2}$ and $^2P_{3/2}$ states of the $^{221}\text{Ra}^+$ ion [19,22].

All the theoretical predictions mentioned above refer to the radium ion. When comparing the calculated contributions of various electron correlation effects in neutral radium and Ra^+ ions, it is important to bear in mind the following considerations. (i) Hyperfine shifts of atomic levels arise primarily due to the interaction of the nuclear magnetic dipole with

the magnetic field generated by the electrons at the site of the nucleus. Usually the large part of the shift is due to different densities of electrons in one or more closed s shells. These differences in densities are induced by the exchange interaction of the valence s electron with only one of the closed-core s -shell electrons (the exchange interaction is zero between electrons with antiparallel spins). To some extent the above applies also to $p_{1/2}$ electrons, since they also have nonzero densities at the site of the nucleus, but the polarization of the core by a valence s electron is much stronger than by a valence $p_{1/2}$ electron. (ii) The valence s electron is absent in the $^2P_{1/2}$ and $^2P_{3/2}$ states of the Ra^+ ion, therefore core-polarization effects should be smaller (in relative terms) than in the $^1,^3P_1$ and 3P_2 states of neutral radium. This is clearly visible in Table II of the present paper, where core polarization (i.e., the difference between the “cv+vv” and “vv” lines) amounts to about 40% of the total A value(s), twice as much as in the case of $^2P_{1/2}$ and $^2P_{3/2}$ states of the Ra^+ ion [22].

On the other hand, the reverse is true with respect to core-core electron correlation effects, i.e., they are much smaller (in relative terms) in neutral radium than in the Ra^+ ion. To get a qualitative understanding of this feature, one has to picture the core-core correlation as a van der Waals-like interaction between the valence electron(s) and the core electrons. The strength of this interaction depends on the dipolar polarizabilities of the interacting shells on one hand, and on the spatial separation between them on the other. It has been shown by Yuan *et al.* [21] that the separation factor leads to a decrease of the core-core correlation contributions to the hyperfine shifts in atoms and ions of the seventh row of the Periodic Table, compared to lighter systems. Qualitatively this can be understood on the grounds that the strength of the van der Waals interaction depends on the sixth power of the distance, and therefore is very sensitive even to small rearrangements in the electronic shell structure of the system in question. This is particularly true in the case of radium, which is one of the biggest atoms in nature. When comparing the relative sizes of the core-core correlation effects in neutral and ionized radium, one has to realize that the radii (i.e., the $\langle r^2 \rangle^{1/2}$ expectation values) of their inner shells are almost identical— $\langle r^2 \rangle^{1/2}(6p) = 2.26$ a.u. in the ion and $\langle r^2 \rangle^{1/2}(6p) = 2.29$ a.u. in the atom—but the radius of the outer $7p$ shell of the Ra^+ ion equals 6.36 a.u., while in the neutral Ra atom this value is 7.83 a.u. Such a difference translates into more than a sixfold decrease of the van der Waals interaction, and into a similar decrease of the core-core correlation contribution to the hyperfine shift, when going from the Ra ion to the atom. It is obviously a very crude estimate (and neglects the fact that there is a second electron in the valence shell of neutral radium) but it does explain the relatively small core-core contributions (i.e., the difference between the “cc+cv+vv” and “cv+vv” lines) in Tables I and II of the present paper.

The effects of the triple substitutions on the magnetic dipole hyperfine structure constants A were estimated by Panigrahy *et al.* [19] to be of the order of 2% for the alkali-like Ra^+ ion. However, the alkali atoms and alkali-like ions are notorious for large third-order correlation effects [28,47], while in the alkaline-earth neutral atoms the third-order ef-

TABLE III. Proposed values of nuclear electric quadrupole moment Q (barn) of ^{223}Ra .

Q (barn)	Method	Reference
1.21 (0.03)	MCDHF	this work
1.254 (0.003) {0.066} ^a	fs Ra II	[15]
1.19 (0.12) ^b	fs Ra I	[12]
1.28	RMBPT	[18]
1.190 (0.007) {0.126}	fs Ra I	[15]
1.2	B(E2)	[11]
1.221	average of all above	

^aQuoted in BNL tables [48] as 1.25 (0.07).

^bStandard value of Raghavan [40].

fects are expected to be much smaller, for the same reason as discussed above (see Ref. [21,18] for qualitative arguments). Also, due to the spin polarization effects, the calculated values of magnetic fields are in general more sensitive to electron correlation effects than electric field gradients. This is clearly reflected when comparing the core-core contributions in Table I (electric field gradients) with those from Table II (magnetic fields) of the present paper. Therefore, we still expect the calculated values of $Q(^{223}\text{Ra})$ to be more accurate than the limit which might arise from the magnetic field calculations alone. However, to take a fully conservative approach, we have estimated the error bar of the final value of Q by assuming the statistical distribution from the magnetic field calculations. This approach yields $Q(^{223}\text{Ra}) = 1.21(0.03)$. This value is compared in Table III with all previous determinations.

Our rather conservative error bar is about twice as small as the previous determination by Neu *et al.* [15]. The two above-mentioned error bars overlap, but their Q value is outside our error limit. Also, our value appears to be closer to their earlier result derived from the measurement of hyperfine structure of the neutral radium, rather than the alkali-like Ra^+ ion. Apparently, the earlier value of Wendt *et al.* [12], $Q(^{223}\text{Ra}) = 1.19(12)$, has also been adopted in the tables of Raghavan [40].

V. CONCLUSIONS

We performed an *ab initio* evaluation of the nuclear electric quadrupole moment of radium-223 isotope. Our final result $Q(^{223}\text{Ra}) = 1.21(0.03)$ fits between the latest values obtained by the group of Wendt [12,15], but has a smaller error bar. The accuracy of the present calculation is limited to a large extent by the available computer power. Further progress is expected from either of the two directions. An increase of the computer power by an order of magnitude would permit a more thorough treatment of the core-core electron correlation effects. Availability of experimentally measured electric quadrupole hyperfine constants B for several other states of radium would permit determination of the radium nuclear electric quadrupole moment with accuracy derived from purely statistical distribution of calculated Q values.

ACKNOWLEDGMENTS

This work was supported by the KBN grant under contract No. 2 P03B 051 22 and by The Academy of Finland, Grants No. 200903 and No. 206102.

-
- [1] R. Lucas, Europhys. News **32**, 5 (2001).
[2] V. V. Flambaum, Phys. Rev. A **60**, R2611 (1999).
[3] K. Jungmann, Acta Phys. Pol. B **33**, 2049 (2002).
[4] V. A. Dzuba, V. V. Flambaum, J. S. M. Ginges, and M. G. Kozlov, Phys. Rev. A **66**, 012111 (2002).
[5] J. S. M. Ginges and V. V. Flambaum, Phys. Rep. **397**, 63 (2004).
[6] I. B. Khriplovich and S. K. Lamoreaux, *CP Violation Without Strangeness* (Springer, Berlin, 1997).
[7] J. Engel, M. Bender, J. Dobaczewski, J. H. de Jesus, and P. Olbratowski, Phys. Rev. C **68**, 025501 (2003).
[8] C. E. Moore, *Atomic Energy Levels*, NSRDS-NBS No. 35 (U.S. GPO, Washington, D. C., 1971).
[9] E. Rasmussen, Z. Phys. **87**, 607 (1934).
[10] H. N. Russell, Phys. Rev. **46**, 989 (1934).
[11] ISOLDE Collaboration, S. A. Ahmad, W. Klempt, R. Neugart, E. W. Otten, K. Wendt, and C. Ekström, Phys. Lett. **133B**, 47 (1983).
[12] K. Wendt, S. A. Ahmad, W. Klempt, R. Neugart, E. W. Otten, and H. H. Stroke, Z. Phys. D: At., Mol. Clusters **4**, 227 (1987).
[13] E. Arnold *et al.*, Phys. Rev. Lett. **59**, 771 (1987).
[14] ISOLDE Collaboration, S. A. Ahmad, W. Klempt, R. Neugart, E. W. Otten, P.-G. Reinhard, G. Ulm, and K. Wendt, Nucl. Phys. A **483**, 244 (1988).
[15] ISOLDE Collaboration, W. Neu, R. Neugart, E. W. Otten, G. Passler, K. Wendt, B. Fricke, E. Arnold, H.-J. Kluge, and G. Ulm, Z. Phys. D: At., Mol. Clusters **11**, 105 (1989).
[16] R. Neugart, E. W. Otten, K. Wendt, S. A. Ahmad, S. N. Panigrahy, R. W. Dougherty, K. C. Mishra, T. P. Das, and J. Andriessen, Hyperfine Interact. **59**, 145 (1990).
[17] V. A. Dzuba, V. V. Flambaum, and O. P. Sushkov, Phys. Scr. **32**, 507 (1985).
[18] J.-L. Heully and A.-M. Mårtensson-Pendrill, Phys. Scr. **31**, 169 (1985).
[19] S. N. Panigrahy, R. W. Dougherty, S. Ahmad, K. C. Mishra, T. P. Das, J. Andriessen, R. Neugart, E. W. Otten, and K. Wendt, Phys. Rev. A **43**, 2215 (1991).
[20] J. Andriessen, H. Postma, and A. M. van den Brink, Phys. Rev. A **45**, 1389 (1992).
[21] X. Yuan, S. N. Panigrahy, R. W. Dougherty, T. P. Das, and J. Andriessen, Phys. Rev. A **52**, 197 (1995).
[22] X. Yuan, R. W. Dougherty, T. P. Das, and J. Andriessen, Phys. Rev. A **52**, 3563 (1995).
[23] I. P. Grant, Comput. Phys. Commun. **84**, 59 (1994).
[24] I. Lindgren and A. Rosén, Case Stud. At. Phys. **4**, 150 (1974).
[25] F. A. Parpia, C. Froese Fischer, and I. P. Grant, Comput. Phys.

- Commun. **94**, 249 (1996).
- [26] P. Jönsson, F. A. Parpia, and C. Froese Fischer, *Comput. Phys. Commun.* **96**, 301 (1996).
- [27] J. Bieroń, P. Jönsson, and C. Froese Fischer, *Phys. Rev. A* **53**, 2181 (1996).
- [28] P. Jönsson, *Phys. Scr.* **48**, 678 (1993).
- [29] C. Froese Fischer and P. Jönsson, *Comput. Phys. Commun.* **84**, 37 (1994).
- [30] T. Brage and C. Froese Fischer, *Phys. Scr., T* **47**, 18 (1993).
- [31] J. Bieroń, P. Pyykkö, D. Sundholm, V. Kellö, and A. J. Sadlej, *Phys. Rev. A* **64**, 052507 (2001).
- [32] J. Bieroń and P. Pyykkö, *Phys. Rev. Lett.* **87**, 133003 (2001).
- [33] J. Bieroń, P. Pyykkö, and P. Jönsson, *Phys. Rev. A* **70**, 012502 (2005).
- [34] B. J. McKenzie, I. P. Grant, and P. H. Norrington, *Comput. Phys. Commun.* **21**, 233 (1980).
- [35] URL physics.nist.gov/cuu/Constants/index.html.
- [36] A. Bohr and F. Weisskopf, *Phys. Rev.* **77**, 94 (1950).
- [37] J. S. Grossman, L. A. Orozco, M. R. Pearson, J. E. Simsarian, G. D. Sprouse, and W. Z. Zhao, *Phys. Rev. Lett.* **83**, 935 (1999).
- [38] J. R. C. López-Urrutia, P. Beiersdorfer, K. Widmann, B. B. Birkett, A.-M. Mårtensson-Pendrill, and M. G. H. Gustavsson, *Phys. Rev. A* **57**, 879 (1998).
- [39] H. Kopfermann, *Nuclear Moments* (Academic Press Inc., New York, 1958).
- [40] P. Raghavan, *At. Data Nucl. Data Tables* **42**, 189 (1989).
- [41] J. Bieroń, C. Froese Fischer, S. Fritzsche, and K. Pachucki, *J. Phys. B* **37**, L305 (2004).
- [42] K. G. Dyall, I. P. Grant, C. T. Johnson, F. A. Parpia, and E. P. Plummer, *Comput. Phys. Commun.* **55**, 425 (1989).
- [43] C. Froese Fischer, T. Brage, and P. Jönsson, *Computational Atomic Structure: An MCHF Approach* (Institute of Physics Publishing, London, 1997), pp. 171-173.
- [44] B. Engels, *Theor. Chim. Acta* **86**, 429 (1993).
- [45] J. Bieroń, P. Jönsson, and C. Froese Fischer, *Phys. Rev. A* **60**, 3547 (1999).
- [46] V. A. Dzuba, V. V. Flambaum, and J. S. M. Ginges, *Phys. Rev. A* **61**, 062509 (2000).
- [47] P. Jönsson, A. Ynnerman, C. Froese Fischer, M. R. Godefroid, and J. Olsen, *Phys. Rev. A* **53**, 4021 (1996).
- [48] URL www2.bnl.gov/ton.